

Synthesis of CdS and ZnS Nanowires Using Single-Source Molecular Precursors

Carl J. Barrelet,[†] Yue Wu,[†] David C. Bell,[‡] and Charles M. Lieber^{*†}

Department of Chemistry and Chemical Biology and Center for Imaging and Mesoscale Structures, Harvard University, Cambridge, Massachusetts 02138

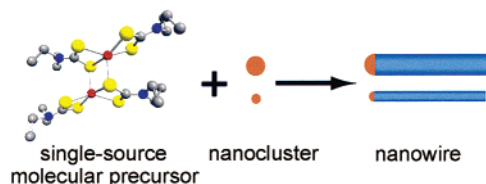
Received July 1, 2003; E-mail: cml@cmliris.harvard.edu

Semiconductor nanowires (NWs) represent a broad class of nanoscale building blocks that have been used to assemble a range of electronic and photonic structures, including light emitting diodes,¹ photodetectors,² and lasers.^{3,4} Critical to the properties and behavior of these and other potential devices are the crystallinity, stoichiometry, and size of the NW building blocks. These key properties can, in principle, be varied during growth, and thus the development of synthetic methods that enable their precise control is expected to have a significant impact on progress. For example, CdS and ZnS NWs, which are direct band-gap semiconductors with attractive photonic properties, have been prepared previously using several approaches including laser-assisted catalytic and vapor-phase growth methods.^{5,6} The laser-based and vapor-phase synthetic methods have demonstrated considerable flexibility in studying a wide range of NW systems; yet the heterogeneous reactants produced by laser ablation and difficulty in controlling nucleation in vapor-phase growth have limited the control of key properties with these methods.

On the other hand, molecular reactants are precisely defined and can thus enable a much higher degree of synthetic control as shown with the growth of silicon and germanium nanowire heterostructures using silane and germane reactants, and the growth of CdSe, CdTe, and InAs nanorods using organometallic sources.^{7,8} Herein, we report the first use of single-source molecular precursors for the growth of CdS and ZnS NWs by a nanocluster-catalyzed vapor–liquid–solid mechanism. By using well-defined molecular reactants, we have been able to prepare in high yield single-crystal nanowires with controlled diameters and high-quality optical properties.

Our synthetic approach (Scheme 1) follows the nanocluster-catalyzed vapor–liquid–solid growth process described previ-

Scheme 1. Nanowire Growth from a Single-Source Molecular Precursor via a Gold Nanocluster-Catalyzed Vapor–Liquid–Solid Mechanism



ously,^{9–11} where $\text{Cd}(\text{S}_2\text{CNET}_2)_2$ and $\text{Zn}(\text{S}_2\text{CNET}_2)_2$ molecular precursors serve as sources for Cd and S or Zn and S reactants, respectively. In this synthetic method, the single-source precursors undergo thermal decomposition in the growth region of a furnace,^{12–14} form M–S–Au (M = Cd or Zn) liquid solutions with the Au nanocluster catalysts, and then undergo nucleation and NW growth when the nanodroplets become saturated with reactant.^{9,10,15,16} All

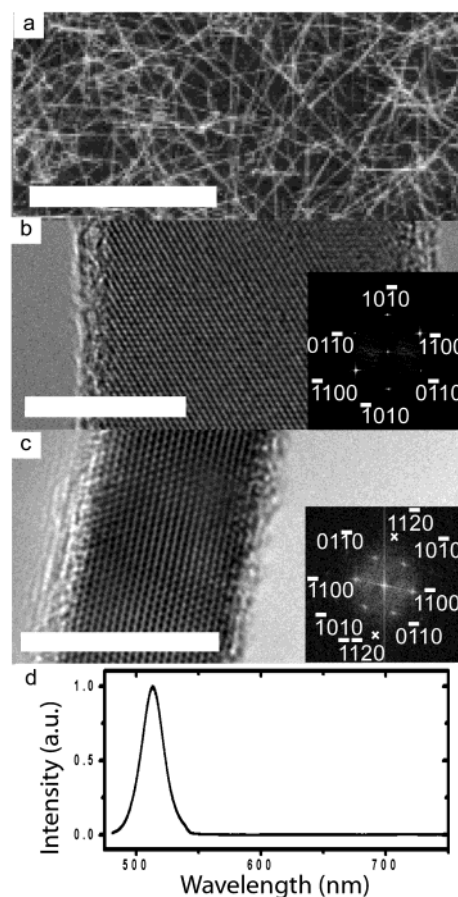


Figure 1. (a) FESEM image of CdS NWs synthesized using 20 nm gold nanoclusters. Scale bar is 10 μm . (b) HRTEM of a 23 nm diameter nanowire grown from 20 nm gold nanoclusters. Scale bar is 10 nm. (inset) Two-dimensional Fourier transform of the TEM image. (c) HRTEM of a 9 nm diameter nanowire grown using 10 nm gold nanoclusters. Scale bar is 10 nm. (inset) Two-dimensional Fourier transform of the TEM image. (d) Photoluminescence spectrum recorded at room temperature on a single 25 nm diameter CdS NW. The NW was excited at 400 nm.

NW synthesis experiments were carried out in a quartz tube heated within a tube furnace using monodisperse gold nanocluster catalysts supported on the oxide surface of SiO_2/Si substrates. The solid molecular precursors were located upstream of the substrates at the entrance to furnace where the lower temperature, 120–180 $^\circ\text{C}$, produced gas-phase reactants without thermal decomposition.

A representative field-emission scanning electron microscopy (FESEM) image of CdS NWs grown using 20 nm diameter catalyst clusters shows that this approach produces NWs in good yield and with uniform ca. 20 nm diameters (Figure 1a). Transmission electron microscopy (TEM) analysis of CdS NW samples prepared from 10 and 20 nm nanoclusters yielded average NW diameters of

[†] Department of Chemistry and Chemical Biology.

[‡] Center for Imaging and Mesoscale Structures.

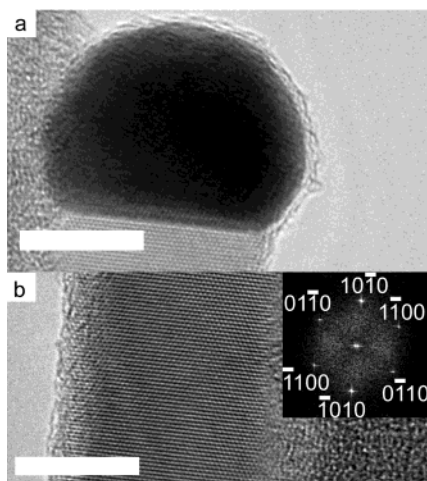


Figure 2. (a) HRTEM of a 17 nm diameter ZnS nanowire grown using 20 nm gold nanoclusters. Scale bar is 10 nm. (b) HRTEM of an 18 nm diameter nanowire grown using 20 nm gold nanoclusters. Scale bar is 10 nm. (inset) Two-dimensional Fourier transform of the TEM image. The lacey carbon substrate is visible to the left and right of the NWs in (a) and (b), respectively.

14 ± 6 and 24 ± 7 nm, respectively, and showed that most NWs terminate at one end with a nanocluster as expected for the growth mechanism (Scheme 1). The good correlation between the NW diameter and the catalyst diameter is consistent with previous studies¹⁰ and is indicative of a well-controlled growth process.

High-resolution TEM (HRTEM) images of representative CdS NWs prepared using 10 and 20 nm diameter nanoclusters show that NWs are single-crystal (Figure 1b,c).¹⁷ The reciprocal lattice peaks, which were obtained by two-dimensional Fourier transform of the lattice resolved images,⁷ can be indexed to a wurtzite (W) structure (insets, Figure 1b,c) with a lattice constant $a = 4.1$ nm. The W-phase is consistent with previous studies of CdS NWs,⁶ thin films prepared using the same precursor,¹⁸ and the stability of W versus zinc blend (ZB) phases.^{8a,c} The indexed reciprocal lattices for the 23 and 9 nm diameter NWs also show that the $[10\bar{1}0]$ and $[11\bar{2}0]$ directions, respectively, are aligned with the NW axes. In addition, energy-dispersive X-ray spectroscopy (EDX) measurements confirm that the composition of CdS NWs is stoichiometric (%Cd = 50.7; %S = 49.3) with no oxygen within the limits (<0.1%) of this technique.

The optical properties of individual CdS NWs have been studied by photoluminescence (PL)^{1,2} to further assess their quality. A representative PL spectrum recorded from a 25 nm diameter NW at room temperature shows a single peak centered at 513 nm, which is consistent with band edge emission, with a full-width at half-maximum (fwhm) of 21 nm (Figure 1d). The relatively narrow fwhm and absence of emission near 600 nm from deep levels associated with defects and impurities¹⁹ demonstrate that these single-crystal NWs have high-quality optical properties and should be good building blocks for photonic structures.

In addition, we have investigated the generality of this approach with the growth of ZnS NWs using $\text{Zn}(\text{S}_2\text{CNET}_2)_2$ as a molecular precursor. TEM structural analyses show that single-crystal ZnS nanowires with controlled diameters are obtained (Figure 2). A TEM image of the nanocluster catalyst at the end of a crystalline ZnS NW (Figure 2a) shows clearly how the nanocluster catalysts define the diameter of NWs. A representative HRTEM image of a 18 nm diameter NW demonstrates that the NW is single-crystal (Figure 2b), and, moreover, the reciprocal lattice peaks can be indexed to a W-structure (inset, Figure 2b) with a lattice constant $a = 3.7$ nm. The indexed reciprocal lattice shows that the $[10\bar{1}0]$ is aligned

with the NW axis. EDX measurements confirm that the composition of ZnS NWs is stoichiometric (%Zn = 49.7; %S = 50.3) with no detectable oxygen. These results thus show that high-quality ZnS NWs can also be prepared by our approach.

In conclusion, we have demonstrated that single-source molecular precursors can be used as well-defined reactants for the synthesis of CdS and ZnS compound semiconductor NWs. The molecular precursors enable controlled diameter growth of single-crystal materials. These high-quality CdS and ZnS NWs represent well-defined nanoscale structures needed both for fundamental optical studies and as building blocks for the assembly of photonic devices.¹⁻⁴ More generally, we believe that our new approach for the growth of II-VI semiconductor NWs opens up the possibility of the well-defined synthesis of metal or chalcogenide alloy NWs, as well as the synthesis of axial and radial NW heterostructures^{1b,7} with novel functions.

Acknowledgment. We thank M. S. Gudiksen, X. Duan, and Y. Cui for helpful discussions. C.M.L. thanks the Air Force Office of Scientific Research for support of this work.

References

- (1) (a) Duan, X. F.; Huang, Y.; Cui, Y.; Wang, J. F.; Lieber, C. M. *Nature* **2001**, *409*, 66–69. (b) Gudiksen, M. S.; Lathon, L. J.; Wang, J.; Smith, D. C.; Lieber, C. M. *Nature* **2002**, *415*, 617–620.
- (2) Wang, J. F.; Gudiksen, M. S.; Duan, X. F.; Cui, Y.; Lieber, C. M. *Science* **2001**, *293*, 1455–1457.
- (3) (a) Huang, M. H.; Mao, S.; Feick, H.; Yan, H. Q.; Wu, Y. Y.; Kind, H.; Weber, E.; Russo, R.; Yang, P. D. *Science* **2001**, *292*, 1897–1899. (b) Johnson, J. C.; Choi, H.-J.; Knutsen, K. P.; Schaller, R. D.; Yang, P.; Saykally, R. J. *Nat. Mater.* **2002**, *1*, 106–110.
- (4) Duan, X. F.; Huang, Y.; Agarwal, R.; Lieber, C. M. *Nature* **2003**, *421*, 241–245.
- (5) Duan, X. F.; Lieber, C. M. *Adv. Mater.* **2000**, *12*, 298–302.
- (6) (a) Ma, C.; Moore, D.; Li, J.; Wang, Z. L. *Adv. Mater.* **2003**, *15*, 228–231. (b) Ye, C.; Meng, G.; Wang, Y.; Jiang, Z.; Zhang, L. *J. Phys. Chem. B* **2002**, *106*, 10338–10341. (c) Wang, Y.; Meng, G.; Zhang, L.; Liang, C.; Zhang, J. *Chem. Mater.* **2002**, *14*, 1773–1777.
- (7) Lathon, L. J.; Gudiksen, M. S.; Wang, D.; Lieber, C. M. *Nature* **2002**, *420*, 57–61.
- (8) (a) Manna, L.; Milliron, D. J.; Meisel, A.; Scher, E. C.; Alivisatos, A. P. *Nat. Mater.* **2003**, *2*, 382–385. (b) Peng, Z. A.; Peng, X. *J. Am. Chem. Soc.* **2001**, *123*, 1389–1395. (c) Manna, L.; Scher, E. C.; Alivisatos, A. P. *J. Am. Chem. Soc.* **2000**, *122*, 12700–12706. (d) Peng, X.; Manna, L.; Yang, W.; Wickham, J.; Scher, E.; Kadavanich, A.; Alivisatos, A. P. *Nature* **2000**, *404*, 59–61. (e) Kan, S.; Mokari, T.; Rothenberg, E.; Banin, U. *Nat. Mater.* **2003**, *2*, 155–158.
- (9) Morales, A. M.; Lieber, C. M. *Science* **1998**, *279*, 208–211.
- (10) (a) Gudiksen, M. S.; Lieber, C. M. *J. Am. Chem. Soc.* **2000**, *122*, 8801–8802. (b) Cui, Y.; Lathon, L. J.; Gudiksen, M. S.; Wang, J. F.; Lieber, C. M. *Appl. Phys. Lett.* **2001**, *78*, 2214–2216.
- (11) The NWs are grown in a flow of 15 sccm of H_2 and 50 sccm of Ar at a pressure of 250 mTorr. The single-source precursor is positioned in the upstream lip of the furnace. A substrate coated with gold nanoclusters is placed in the downstream lip of the furnace.
- (12) Sharma, A. K. *Thermochim. Acta* **1986**, *104*, 339–372.
- (13) O'Brien, P.; Nomura, R. *J. Mater. Chem.* **1995**, *5*, 1761–1773.
- (14) Fainer, N. I.; Kosinova, M. L.; Romyantsev, Y. M.; Salman, E. G.; Kuznetsov, F. A. *Thin Solid Films* **1996**, *280*, 16–19.
- (15) Wu, Y. Y.; Yang, P. D. *J. Am. Chem. Soc.* **2001**, *123*, 3165–3166.
- (16) Detailed information on ternary phase diagrams of Au–Cd–S and Au–Zn–S relevant to the VLS mechanism is unavailable to our knowledge. The growth temperature range used for single-source precursors (for CdS, 750–850 °C, and for ZnS, 850–1000 °C) is similar to the one reported for laser-assisted catalysis growth (for CdS, 790–870 °C, and for ZnS, 990–1050 °C).
- (17) For HRTEM imaging, the NWs were suspended in ethanol, dispersed onto a lacey carbon film substrate (Ted Pella), and imaged with a JEOL 2010F TEM with an accelerating voltage of 200 kV.
- (18) Pike, R. D.; Cui, H.; Kershaw, R.; Dwight, K.; Wold, A.; Blanton, T. N.; Wernberg, A. A.; Gysling, H. J. *Thin Solid Films* **1993**, *224*, 221–226.
- (19) Bagnall, D. M.; Ullrich, B.; Sakai, H.; Segawa, Y. *J. Cryst. Growth* **2000**, *214*, 1015–1018.

JA036990G